Integrated optic beam combiners for astronomic interferometry: rapid prototyping of hybrid sol-gel devices

A. Ghasempour[1,2,4], D. Alexandre[1,2,3], C. Brites[1,2], P.J. Moreira[1,4], P.J.V. Garcia[4,5], J. L. Santos[1,2], P.V.S. Marques[1,2] and A.M.P Leite[2]

[1]Unidade de Optoelectrónica e Sistemas Electrónicos – INESC Porto, Portugal
[2]Departamento de Física da Faculdade de Ciências da Universidade do Porto, Portugal
[3]Departamento de Física da Universidade de Trás-os-Montes e Alto Douro, Portugal
[4]Centro de Astrofísica da Universidade do Porto, Portugal
[5]Departamento de Engenharia Física da Faculdade de Engenharia da Universidade do Porto, Portugal

Abstract: *Results concerning the design, fabrication and characterization of a multiaxial two beam combiner for astronomical interferometry are presented. The devices were fabricated in hybrid sol-gel materials in conjunction with laser direct writing techniques.*

1. Introduction

Long baseline optical (1μm<λ<10μm) astronomical interferometry is an emerging technology allowing angular resolutions an order of magnitude larger than the largest available telescopes [1]. Existing arrays, with telescopes separated by 200m baselines, are able to reach angular resolutions in the near infrared (λ~1μm) of the order of 5 pico-radians. In contrast, the largest telescopes (10m diameter) only reach 0.1 μradians. As the technology matures the number of telescopes in the arrays increases and instruments are now under design to combine up to 8 telescopes [2]. Single mode guided wave optics has a great potential for the implementation of several critical functions (e.g. beam transportation, equalization, combination and metrology) for these broadband single mode interferometers both in ground [3] and space [4]. Integrated optics beam combination devices can be implemented using different basic schemes [3]. The coaxial combination arrangement (similar to the configuration of the Michelson interferometer) can be implemented with cascaded Y-junctions [5], for field splitting and combination. The multiaxial combination scheme (similar to that of the classical Young's interferometer) can be constructed through angularly coded propagation of nearly collimated guided waves in planar waveguide sections [6], as discussed below. Photometry channels can be included to allow for the correction of the interferometric raw signals in terms of unequal beam powers due to atmospheric thurbulence. The interferometer arrangements can vary from "pair-wise" to "all-in-one" combination [10]. Fundamental aspects, such as preservation of polarization and broadband response have to be taken into account in the guided wave designs.

Co-axial beam combiners demonstrators at H (λ~1.6μm) and K (λ~2.2 μm) astronomical bands have been fabricated with ion-exchange in glass and silica-on-silicon technologies [5, 7, 8], some including metrology functions integrated with the science beam combiner [9]. In this paper we focus on the fabrication of a multi-axial beam combiner using hybrid sol-gel technology for the J astronomical band (λ~1.2 μm).

2. Hybrid sol-gel technology

The hybrid sol-gel technology offers an interesting potential for simplified fabrication and rapid prototyping of integrated optic devices [11], as low temperature processing is used, thick optical layers can be achieved in a single deposition and no reactive ion etching is needed. Using the MAPTMS-ZrO_2 material system and UV laser patterning, channel waveguides and devices have been demonstrated, without recourse to photoinitiator [12]. As this material system allows direct photopatterning, it is quite suitable for testing of designs and verification of concepts.

A laser photopatterning system has been developed which can produce masks on special plates with a focussed laser beam (532 nm), or write directly the integrated optic hybrid sol-gel device using a UV laser (244 nm). The laser writer is computer controlled, uses the output CAD files from an integrated optics simulation package, and the pattern is written by X-Y displacement of crossed precision translation stages (2nm resolution) under the dynamically focussed laser beam. Figure 1 shows the laser direct writing machine developed and the multiaxial two beam combiner produced.

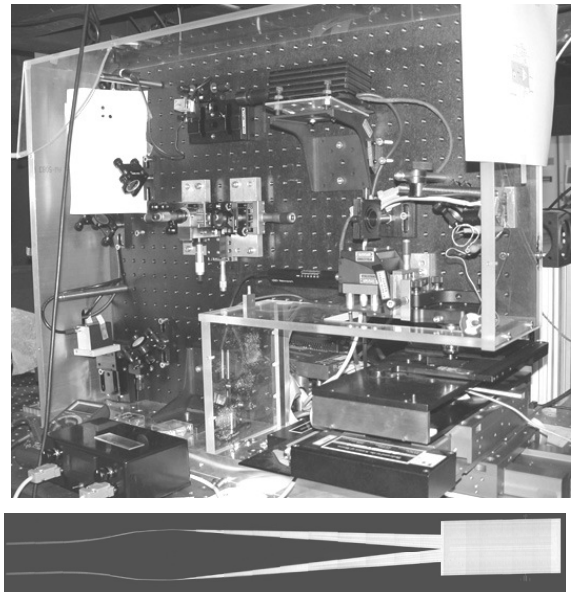

Figure 1 – Photograph of the laser direct writing unit and picture of the multiaxial two beam combiner written in mask photoblanks

Loss levels measured on single mode sol-gel channel waveguides are 0.4dBcm^{-1} @ 1300 nm, which are acceptable from the point of view of rapid prototyping. High performance devices should, however, employ lower loss silica waveguides, but their design follows very similar rules to those applied in the sol-gel case.

3. Design of integrated optics beam combiners

The design of the prototypes of several configurations of coaxial and multiaxial beam combiners for the J band used a BPM-CAD commercial software package (Optiwave). Channel waveguides were designed with a square core (typically $4\times4\,\mu m^2$) to guide a single mode and couple efficiently to single mode fibres. Elements such as S-bends, X-crossings, Y-junctions and waveguide tapers were individually studied and optimized. Figure 2 shows the amplitude of the field in a coaxial two beam combiner with photometry outputs, based on Y-junctions.

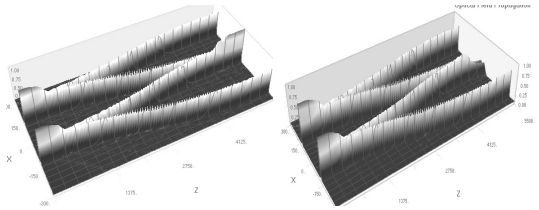

Figure 2 – Field amplitude along the two beam combiner for inputs in phase and π out of phase.

For an even number N of input beams, the design of a coaxial all-in-one beam combiner follows almost directly from the design for N=2. However, in the case of N odd, the design is slightly more complex, as it is of fundamental importance to ensure that all interfering optical paths have the same length for correct broadband operation.

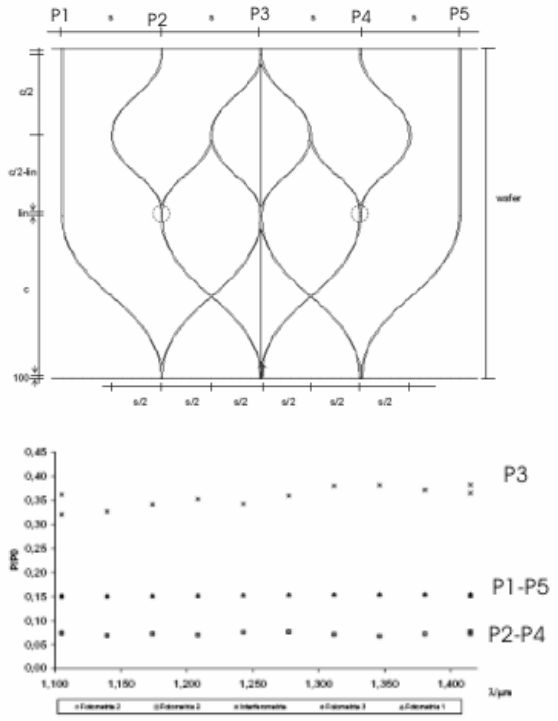

Figure 3 – (a) Schematic layout of a three beam combiner and (b) power output as a function of wavelength.

Figure 3 shows the layout for a N=3 device with photometry outputs, and the results of its simulation.

The design of multiaxial combiners was also addressed, and Figure 4 displays a configuration for N=3. Waveguide tapers are employed to achieve adiabatic expansion of the square core channel waveguide field to the fundamental mode of a rectangular core waveguide at the taper end ($150\times4\mu m^2$), in order to ensure nearly collimated beams in the planar waveguide section. The taper axis angles δ_i must be chosen carefully in order to result in interference fringe patterns with different periods for each beam pair combination, in order to discriminate between the interferometric spatial patterns. The radius R of the planar waveguide region and the angular separation of the taper ends must ensure that no coupling occurs between neighbour waveguides.

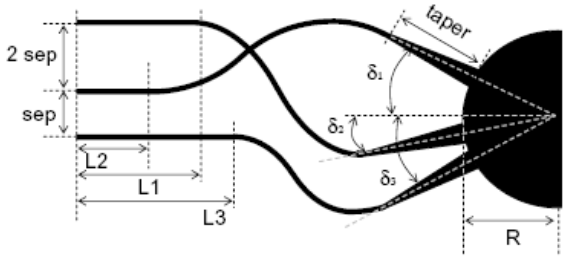

Figure 4 – Schematic representation of a multi-axial beam combiner (in this case, $\delta_1 > 0, \delta_{2,3} < 0$).

The spatial frequency f_{ij} of the pattern for the (i, j) beam pair is given by

$f_{ij} = C\left|\sin\delta_i - \sin\delta_j\right|$, where $C = n_{eff} / \lambda_0$, n_{eff} is the effective index of the fundamental mode in the planar region and λ_0 is the vacuum wavelength. The spatial frequencies can be arranged in a $1f_0$, $2f_0$, $3f_0$ series, where f_0 is the lowest frequency (which depends on the specification of the transverse magnification M_T of the optical system used for fringe detection, and on the CCD detector pixel period d_{pixel}; the maximum frequency $3f_0$ should be $M_T / 2d_{pixel}$ in order to achieve accurate recording of the pattern). Additional information is necessary to calculate a unique solution; the criterion used was to specify a symmetric angular aperture to cover all taper axes (in this example, $\delta_1 = -\delta_3$), resulting in

$$\delta_1 = -\delta_3 = \arcsin\left[\frac{3\lambda_0 f_0}{2n_{eff}}\right]; \delta_2 = -\arcsin\left[\frac{\lambda_0 f_0}{2n_{eff}}\right]$$

Figure 5 shows the layout of a 2 beam combiner and respective field distribution in the interference region. Photometry outputs were not included, but were used in other designs. Particular care was taken in the design of S-bends to avoid field distortion at the tapers inputs.

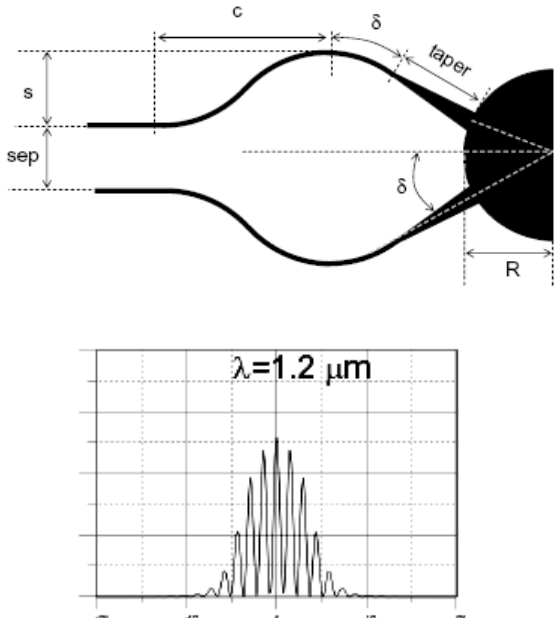

Figure 5 – Schematic representation of a two beam combiner and intensity distribution at the output plane.

The modal field amplitudes have a distribution which causes modulation of the fringe pattern, as shown in Figure 5. This implies a certain spatial frequency bandwidth for each interference pattern, thus forcing a minimum separation between the centre frequencies ($n\times f_0$) of the fringe patterns in order to separate them in the signal processing stage, for N>2.

The N=3 combiner design presents more problems, as the channel waveguides feeding the tapers must provide optical path equalization over the specified radiation bandwidth in order to keep the white-light fringe well centred and maximum for equal input

phases. This resulted in the design of Figure 4, which employs an X-crossing and adjustment of the input fibre positions.

4. Experimental results

The production of a master mask used a Canyon Materials Inc photomask blank and laser direct writing (532nm). Amplitude masks were subsequently replicated on fused silica substrates, using standard lithography techniques.

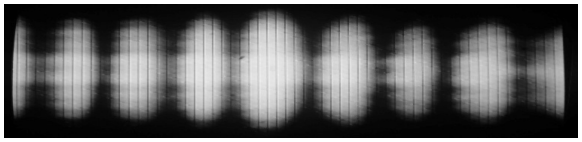

Figure 6 – Experimental intensity pattern at device output imaged in the sensor of a vidicon camera using a 4× microscope objective lens, using a semiconductor laser at 1.3μm. The spatial period is ≈ 20.5μm, in good accordance with the expected value (20.0μm). The vertical lines are an artefact of the image.

The sol-gel core layer is 4 μm thick, and was deposited on soda-lime substrates using spin coating (n_{core}=1.5076.@ λ_0=1302 nm). The cladding layer (n_{clad}=1.4976.@ λ_0=1302 nm) was also deposited by spinning, and has a thickness of 15μm. The detailed fabrication procedure is described in [12].

Coaxial all-in-one two and three beam combiners, and a two beam multiaxial device, were fabricated and tested for their basic functionality. Figure 6 shows the example of the output fringe pattern obtained from the multiaxial device at λ=1.3μm, as captured using a 4× microscope objective at a distance of 138 cm from an infrared camera linked to an image processing system. The spatial period measured is 20.5 μm, in good agreement with the calculated value. Further tests are under way in this and other devices, in order to extract data on polarization and chromatic performance.

5. Conclusions

We presented the first fabrication of multiaxial beam combiners using hybrid sol-gel technology. Their optical properties open the possibility of using these devices in the J astronomical band. The combination of an integrated optics simulation-CAD package with a laser writing machine, linked to the use of hybrid sol-gel technology, provides a useful solution to rapid prototyping of complex integrated optic devices, such as beam combiners used in astronomic interferometry. Design considerations were adressed and experimental results of a multiaxial two beam combiner were presented. Other implementations are presently under investigation.

Acknowledgments

AG is supported by a doctoral fellowship SFRH/BD/24493/2005 approved by FCT and POCI, with funds from the European community programme FEDER. This work was partially supported by the EU FP6 under contract number RII3-Ct-2004-001566 (OPTICON).

References

1. Monnier J.D., Rep. Prog. Phys. **66**, 789-857 (2003).
2. Malbet, F. et al., in proceedings of SPIE **5491**. Edited by Wesley A. Traub, pag. 439 (2004)
3. Malbet F., et al, Astron. Astrophys. Suppl. Ser. 138, 135-145 (1999).
4. Olivier S., et al, J. Opt. A: Pure Appl. Opt. **7**, 660-662 (2005).
5. Berger J.P., et al, Astron Astrophys. Suppl. Ser. **139,** 173-177 (1999).
6. Schanen-Duport I., et al, Appl. Opt. **33,** 5954-5958 (1994).
7. LeBouquin J.-B., et al, Astron. Astrophys. **424**, 719-726 (2004).
8. LeBouquin J.-B., et al, Astron. Astrophys. **450**, 1259-1264 (2006).
9. Collomb V., et al, ECIO'05, post-deadline paper (2005).
10. LeBouquin J.-B., Proc. SPIE **5491**, 1362-1369 (2004).
11. Andrews M.P., Najafi S.I., (eds), SPIE **CR-68** (1997).
12. Moreira P.J., et al, Phot. Technol. Lett. **17**, 399-401 (2005).